

---

# Dropout Strikes Back: Improved Uncertainty Estimation via Diversity Sampling

---

Evgenii Tsymbalov\*, Kirill Fedyanin\* and Maxim Panov  
Skolkovo Institute of Science and Technology (Skoltech)  
Moscow, Russia

## Abstract

Uncertainty estimation for machine learning models is of high importance in many scenarios such as constructing the confidence intervals for model predictions and detection of out-of-distribution or adversarially generated points. In this work, we show that modifying the sampling distributions for dropout layers in neural networks improves the quality of uncertainty estimation. Our main idea consists of two main steps: computing data-driven correlations between neurons and generating samples, which include maximally diverse neurons. In a series of experiments on simulated and real-world data, we demonstrate that the diversification via *determinantal point processes*-based sampling achieves state-of-the-art results in uncertainty estimation for regression and classification tasks. An important feature of our approach is that it does not require any modification to the models or training procedures, allowing straightforward application to any deep learning model with dropout layers.

## 1 Introduction

Uncertainty estimation (UE) recently become a very active area of research in deep learning. Neural networks usually are treated as black boxes, and in general, they are prone to overconfidence [Guo et al., 2017, Gal, 2016]. Uncertainty estimation methods aim to help overcome this drawback by identifying potentially erroneous predictions. This can be especially important for error-critical applications like medical diagnostics [Begoli et al., 2019] or autonomous car driving [Feng et al., 2018].

Another important application for uncertainty estimation is active learning [Settles, 2012]. In active learning, we have a relatively small training set and a large unlabeled pool set. Labeling samples from the pool is supposed to be expensive, for example, manual labeling of images or accurate calculation of molecular energies with quantum mechanical models. Thus, it becomes critical to sample points in a way to obtain the most substantial improvement in model quality. The majority of sampling criteria in active learning are based on estimates of uncertainty, which makes it important to obtain high-quality uncertainty estimates.

There are several main approaches for uncertainty estimation for deep neural networks. Bayesian neural networks (BNN) and variational inference in particular represent a natural way for uncertainty estimation due to availability of well-defined posteriors, but they can be prohibitively slow for large-scale applications. The usage of dropout at the inference stage was shown to be good and efficient approximation to BNNs [Gal and Ghahramani, 2016, Gal, 2016]. The ensembles of independently trained models [Lakshminarayanan et al., 2017] have state-of-the-art performance in many tasks requiring uncertainty estimation [Snoek et al., 2019]. Recently, forcing models in ensembles to be more diverse was shown to improve results even further [Jain et al., 2019]. The drawback of

---

\*Equal contribution.

ensembles is that we need to train and use multiple models that require additional resources, i.e. more memory to store models and more computing power for training.

In this work, we aim to develop a new approach for dropout-based uncertainty estimation. Usually there are many highly correlated neurons in neural networks, which results in a slow convergence of estimates based on the standard uniform sampling in dropout layers. We propose to estimate correlations between neurons based on the data and sample the most diverse neurons in order to improve the convergence of the estimates and, as a result, the quality of uncertainty estimates. As a particular realization of the general idea, we suggest sampling dropout masks using the machinery of determinantal point processes (DPP) [Macchi, 1975, Kulesza et al., 2012] which are known to give diverse samples.

We summarize the main contributions of the paper as follows:

- We propose two DPP-based sampling methods for neural networks with dropout. Our approach requires to train only a single model and adds only small overhead on the inference stage compared to plain MC dropout.
- We compare different dropout-based approaches for uncertainty estimation in an extensive series of experiments for real-world regression and classification datasets. The results show superior performance of proposed DPP-based approaches.
- Importantly, the proposed methods show high quality of uncertainty estimation even for very small number of stochastic passes through the network, thus opening the possibility to significantly speed up the inference stage.

The rest of the paper is organized as follows. Section 2 introduces the proposed method for DPP-based sampling from neural networks with dropout. In Section 3, we show the efficiency of the proposed approach in the problem of uncertainty estimation. Section 4 gives an overview of the related work on uncertainty estimation for neural networks. Section 5 concludes the study and highlights some directions for future work.

## 2 Methods

### 2.1 Neural Networks with Dropout as Implicit Ensembles

We start by considering a standard fully connected layer in a neural network

$$S_i^h = \sum_{j=1}^{N_{h-1}} w_{ij}^h O_j^{h-1}, \quad i = 1, \dots, N_h, \quad (1)$$

where  $O_i^h = \sigma(S_i^h)$  is an output of the  $h$ -th layer of the neural network given by a non-linear transformation  $\sigma(\cdot)$  of the corresponding pre-activation  $S_i^h$ . An application of dropout to neurons results in the following formula for the pre-activations:

$$S_i^h = \sum_{j=1}^{N_{h-1}} \frac{1}{1-p} m_j^h w_{ij}^h O_j^{h-1}, \quad i = 1, \dots, N_h, \quad (2)$$

where  $m_j^h$  are Bernoulli random variables with a probability of 0 equal to  $p$ . The outputs  $O_i^h$  of the  $h$ -th layer remain to be computed by  $O_i^h = \sigma(S_i^h)$ . Note that if an input variable of neural network is denoted by  $\mathbf{x}$ , then then output of every layer is a function of  $\mathbf{x}$ , i.e.,  $O_i^h = O_i^h(\mathbf{x})$ .

Let us denote the vector of dropout weights  $m_j^h$  for the  $h$ -th layer by  $\mathbf{m}_h = (m_1^h, \dots, m_{N_h}^h)^T$  and the full set of dropout weights by  $\mathbf{M} = (\mathbf{m}_1, \dots, \mathbf{m}_K)$ . Thus, any neural network  $\hat{f}(\mathbf{x})$  with dropout layers essentially has two sets of parameters: the full set of learnable weights  $\mathbf{W}$  and the set of dropout weights  $\mathbf{M}$ :

$$\hat{f}(\mathbf{x}) = \hat{f}(\mathbf{x} \mid \mathbf{W}, \mathbf{M}).$$

Let us have a neural network with dropout, which was trained on some dataset giving weight estimates  $\hat{\mathbf{W}}$ . Then dropout weights  $\mathbf{M}$  can be considered as free parameters and require selection at the time

of inference

$$\hat{f}(\mathbf{x} | \mathbf{M}) = \hat{f}(\mathbf{x} | \hat{\mathbf{W}}, \mathbf{M}).$$

The originally proposed [Hinton et al., 2012] and currently the standard choice is to take  $\hat{\mathbf{M}} = (1 - p) \cdot \mathbf{E}$ , where  $\mathbf{E}$  is the matrix of all ones of the corresponding shape. Such an approach gives the fixed function  $\hat{f}(\mathbf{x} | \hat{\mathbf{M}})$ , which is known to give reasonably good performance in practice. The main intuition behind such choice is the replacement of the stochastic pre-activations  $S_i^h$  given by (2) with their expectations, which are exactly equal to (1).

Recently, it was proposed to consider dropout as a variational approximation in a specially chosen Bayesian model, see [Gal and Ghahramani, 2016]. Within this approach, one can sample  $T$  i.i.d. realizations  $\mathbf{M}_1, \dots, \mathbf{M}_T \sim \text{Bernoulli}(1 - p)$  and compute approximate posterior mean and variance

$$\bar{f}_T(\mathbf{x}) = \frac{1}{T} \sum_{i=1}^T \hat{f}(\mathbf{x} | \mathbf{M}_i), \quad \bar{\sigma}_T^2(\mathbf{x}) = \frac{1}{T} \sum_{i=1}^T (\hat{f}(\mathbf{x} | \mathbf{M}_i) - \bar{f}_T(\mathbf{x}))^2.$$

The approximate posterior variance  $\bar{\sigma}_T^2(\mathbf{x})$  is a natural choice for the uncertainty estimate and was successfully used in the variety of applications such as out-of-distribution detection [Vyas et al., 2018] and active learning [Gal et al., 2017].

In this paper, we suggest a different approach, namely we treat  $\hat{f}(\mathbf{x} | \mathbf{M})$  as an ensemble of models indexed by dropout masks  $\mathbf{M}$ . Such a view allows us to decouple inference from training and pose an intuitive question: what set of masks  $\mathbf{M}_1, \dots, \mathbf{M}_T$  should one choose in order to obtain the best uncertainty estimate  $\bar{\sigma}_T^2(\mathbf{x})$ ?

Importantly, here we do not limit the selection of masks to be samples from standard dropout distribution, which, in principle, should allow us to obtain better estimates. However, the design of mask selection procedure is a non-trivial problem, which we discuss below in detail.

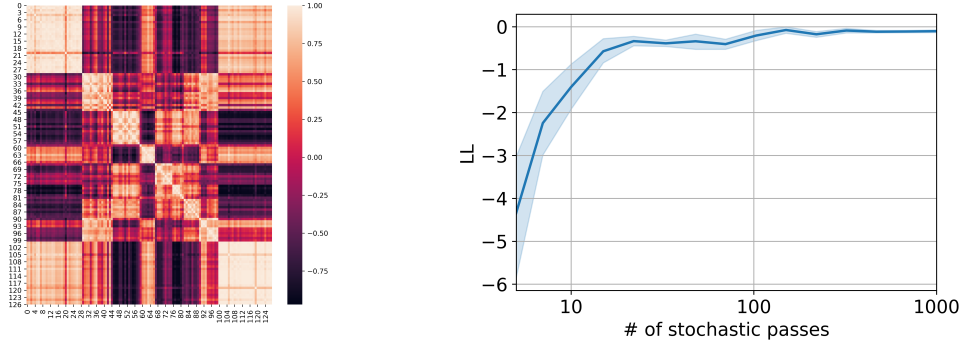
**Remark 1** *The standard approach in the literature is to consider an ensemble of models trained on different subsets of the data set or just from different random initializations giving the set of parameter estimates  $\hat{\mathbf{W}}_1, \dots, \hat{\mathbf{W}}_T$  and corresponding approximations  $\hat{f}(\mathbf{x} | \hat{\mathbf{W}}_i, \hat{\mathbf{M}})$ ,  $i = 1, \dots, T$ . Similarly, one can compute the variance  $\bar{\sigma}_T^2(\mathbf{x})$ , which was shown to be a reasonable uncertainty estimate in practice [Smith et al., 2018, Beluch et al., 2018]. The main drawback of this approach is the need to train and store  $T$  different models, which might be very costly both in terms of computation and storage needed.*

## 2.2 Data-driven Mask Generation Under General Sampling Distributions

In practice, many neurons in the network are highly correlated. For example, consider a correlation matrix of neurons in a hidden layer of a fully-connected neural network, trained on the regression dataset (see Figure 1a). The correlation matrix was computed on the test set and clearly shows groups of highly correlated neurons. Sampling masks for this layer uniformly at random might result in a high variance of pre-activations (2). As a result, the estimates for the whole network may require a significant number of samples (stochastic passes through the NN)  $T$  to converge. We illustrate this behaviour on Figure 1b, where several hundreds of simple MC dropout estimates are required for the convergence of the log-likelihood values. It is clearly seen that a larger number of samples improves the values of log-likelihood, yet may impose computational cost too large to be used in real-world applications. However, one may expect that the knowledge about the correlations between neurons can help to sample more diverse neurons and improve the estimates.

In what follows, we consider the probabilistic generation of masks  $\mathbf{m}_h$  from some distribution  $P^{(h)}$  with possibly non-i.i.d. distributions of components. Similarly to the case of dropout, we suggest using an unbiased estimate of the layer-wise mean. Our main motivation is to approximately preserve the average performance of the trained network. The construction of the unbiased estimator is non-trivial and is given by celebrated Horvitz-Thompson (HT) estimator [Horvitz and Thompson, 1952]:

$$S_i^h = \sum_{j=1}^{N_{h-1}} \frac{1}{\pi_j^h} m_j^h w_{ij}^h O_j^{h-1}, \quad i = 1, \dots, N_h, \quad (3)$$



(a) Correlation matrix.

(b) Log-likelihood for MC dropout as a function of  $T$ .

Figure 1: **(a)** Correlation matrix  $C$  between the outputs of the neurons in a hidden layer of the NN trained on the *naval propulsion* dataset. **(b)** For the same dataset log-likelihood computed via MC dropout increases with increase of the number of stochastic passes  $T$ . More than 100 samples are needed to reach convergence.

where  $\pi_j^h$  is the marginal probability of value 1 for the random variable  $m_j^h$ .

### 2.3 Diversity Sampling Approaches

Let us consider  $h$ -th hidden layer of the neural network with dropout. Assume that we have access to the correlations

$$C_{ij}^{(h)} = \text{corr}_{\mathbf{x}}\{O_i^h(\mathbf{x}), O_j^h(\mathbf{x})\}, \quad i, j = 1, \dots, N_h.$$

In practice, we compute an empirical correlation based on some set of points, which represents the data distribution well enough. As a result, we obtain the correlation matrix  $C^{(h)} \in \mathbb{R}^{N_h \times N_h}$  between the neurons of the  $h$ -th hidden layer. Below we discuss several approaches to sampling neurons in a way that the correlation between sampled neurons is as small as possible. We note that instead of the correlation matrix  $C^{(h)}$  one may consider the covariance matrix  $K^{(h)}$  in any of the approaches described below. The properties of the methods significantly depend on the choice of the matrix, and we will perform the empirical evaluation of the methods based on each of them in the experiments.

#### 2.3.1 Leverage Score Sampling

A basic approach for non-uniform sampling of rows and columns in kernel matrices is the so-called *leverage score sampling* [Alaoui and Mahoney, 2015]. In this approach, the neurons are sampled independently with different probabilities  $\pi_j^h$ :

$$\pi_j^h \sim \ell_\lambda^{(h)}(j) = \left[ C^{(h)} (C^{(h)} + \lambda I)^{-1} \right]_{jj}, \quad j = 1, \dots, N_h,$$

where the quantities  $\ell_\lambda^{(h)}(j)$  are called *leverage scores*. This approach makes neurons from large and highly correlated clusters to be sampled less frequently. In Section 3, we show that leverage score sampling indeed allows obtaining better uncertainty estimates for out-of-distribution data in regression tasks compared to MC dropout. However, its performance for in-domain data is even inferior to uniform sampling. In the next section, we propose a more complex approach, which allows to significantly improve the quality of uncertainty estimation.

#### 2.3.2 Sampling with Determinantal Point Processes

Determinantal Point Processes (DPPs) [Kulesza et al., 2012] are specific probability distributions over configurations of points that encode diversity through a kernel function. They were introduced in [Macchi, 1975] for the needs of statistical physics and were used for a number of ML

applications, see [Kulesza et al., 2012] for an overview. DPP can be seen as a probabilistic MaxVol algorithm [Goreinov et al., 2010, Çivril and Magdon-Ismael, 2009] of finding a maximal-volume submatrix.

We use correlation matrix  $C^{(h)}$  as the likelihood kernel for DPP. Then, given a set  $S$  of selected points for a mask distribution  $\mathbf{m}_h \sim DPP(C^{(h)})$ , we obtain

$$\mathbb{P}[\mathbf{m}_h = S] = \det \left[ C_S^{(h)} (C^{(h)} + I)^{-1} \right], \quad h = 1, \dots, K,$$

where  $C_S^{(h)} = \left[ C_{ij}^{(h)}, i, j \in S \right]$ , i.e., a square submatrix of  $C^{(h)}$  obtained by keeping only rows and columns indexed by  $S$ .

To better understand the DPP, let us come back to the correlation matrix depicted in Figure 1a. The probability for DPP to take highly correlated neurons into the sample  $S$  is low as, in this case, the corresponding determinant  $\det C_S^{(h)}$  will have a small value. Thus, DPP tends to sample neurons from different clusters, increasing an overall diversity.

From computational point of view, DPP-sampling requires  $O(N_h^3)$  operations for generating each sample. It is quite expensive but completely viable even for modern large networks which usually have up to 1024 neurons in fully-connected layers. Importantly, masks can be precomputed once, and then the same masks are used on the inference stage for every test sample with no additional overhead. Also, computations in last fully-connected layers with dropout usually require only few percents of the total computational budget in ImageNet-size networks. Therefore, a computational overhead caused by the DPP-sampling does not have a significant impact on the inference time.

### 2.3.3 k-DPP

The k-DPP [Kulesza et al., 2012] is a variation of the DPP, conditioned to produce samples of fixed size  $|S| = k$ . With the cost of introducing an additional parameter, it allows us to tune the sampling procedure as the choice of  $k$  apparently has a significant influence on the result. In this work, we use for the  $h$ -th layer  $k^{(h)} = (1 - p)N_h$ , so that the number of neurons in the sample is equal to the mean number of neurons in the sample of MC-Dropout. In the case of k-DPP, the computation of the marginal probabilities  $\pi_j^h$  for HT-estimator (3) is non-trivial and requires the separate optimization procedure, see the details in [Amblard et al., 2018].

## 2.4 Diversification for Uncertainty Estimation in Classification

For regression, the variance of prediction is a standard uncertainty measure. However, uncertainty estimation for classification is, in some sense, more challenging than for regression as there is no obvious candidate for uncertainty measure.

Let us define the average probability for the class prediction by ensemble members  $\bar{p}_T(y = c | \mathbf{x}) = \frac{1}{T} \sum_{i=1}^T p(y = c | \mathbf{x}, \mathbf{M}_i)$ . The standard uncertainty measure usually considered in the literature is

$$s(\mathbf{x}) = 1 - \max_c \bar{p}_T(y = c | \mathbf{x}),$$

which is based solely on the mean probabilities predicted by the ensemble. While providing good results in practice [Snoek et al., 2019, Ashukha et al., 2020] it doesn't use the information about the variation of predictions between ensemble members.

In our work, we consider *BALD* [Houlsby et al., 2011] uncertainty measure and combine it with different sampling schemes considered above. BALD is equal to the mutual information between outputs and model parameters:

$$I(\mathbf{x}) = H(\mathbf{x}) - \frac{1}{T} \sum_{c=1}^C \sum_{i=1}^T -p(y = c | \mathbf{x}, \mathbf{M}_i) \log(p(y = c | \mathbf{x}, \mathbf{M}_i)),$$

where  $H(\mathbf{x}) = -\sum_{c=1}^C \bar{p}_T(y = c | \mathbf{x}) \log(\bar{p}_T(y = c | \mathbf{x}))$  is an entropy of the ensemble mean. Importantly, BALD values are directly linked with the diversity of the ensemble members, and

Table 1: Summary of the UCI datasets used in experiments, see [Dua and Taniskidou, 2017].

Dataset name	naval propulsion	concrete	boston housing	kin8nm	ccpp	red wine
Samples	11934	1030	506	8192	9568	1599
Features	16	8	13	8	4	11

therefore are well suited for combination with our approach. The other viable alternative is the so-called *variation ratio* uncertainty measure [Freeman, 1965], see additional experiments with it and with  $s(\mathbf{x})$  in Supplementary Material.

### 3 Experiments

#### 3.1 Uncertainty Estimation for Regression

##### 3.1.1 Models and Metrics

For the experiments, we consider MC dropout as a baseline and all the proposed UE methods discussed in the Section 2.3: leverage score sampling, DPP and k-DPP. We present the results for leverage score sampling and DPP based on correlation matrix and k-DPP based on covariance matrix as such a choices give consistently better results compared to an alternative (see Supplementary Material for the results of other combinations). For leverage score sampling we deliberately choose  $\lambda = 1$  to make it working with de-facto the same matrix as DPP-based methods. We used feed-forward NNs with 3 hidden layers (128-128-64 neurons) and leaky ReLU activation function [Maas et al., 2013]. For DPP-based methods, we use the DPPy implementation provided in [Gautier et al., 2019]. Additional details on model architectures and training procedures can be found in Supplementary Material.

We should note that we do not compare with fully Bayesian approaches as we are focusing on the solutions applicable to the standard dropout-based models without changing model architecture and training procedure. Following [Hernández-Lobato and Adams, 2015, Jain et al., 2019], we use log-likelihood of Gaussian distribution with mean and variance computed by different methods as a quality measure.

On top of single models, we also consider a straightforward ensemble approach with NNs trained exactly the same way as single models but from different random initializations. Our experiments show that uncertainty estimates based on ensembling of networks without sampling in individual networks doesn't work for well for the considered regression datasets. However, in Supplementary Material we show that combining ensembling with sampling can further improve the results compared to single models.

##### 3.1.2 Experiments on Regression Datasets

Similarly to [Jain et al., 2019], we run a series of experiments on various regression datasets, see Table 1 for the full list of datasets. We start with in-domain uncertainty estimation: for each dataset, random 50% of points were used for training and other 50% for testing. The log-likelihood values are averaged over testing set. Multiple experiments are done via 5 random train-test splits, 2-fold cross-validation and 5 runs of the training procedures for every model (resulting in 50 average log-likelihood values contributing to each boxplot). Uncertainty estimates were computed for different number of stochastic passes  $T = 10, 30$  and 100 for every model.

We show the resulting distributions of log-likelihood values for each dataset on Figure 2. We observe that either DPP or k-DPP always show the best results. Most importantly, DPP works very well already for small number of stochastic passes  $T = 10$  and consistently has low variance which is extremely important for practical usage. For the additional results concerning ensembles of models and different variations of NNs, see Supplementary Material.

We also performed an experiment with out-of-distribution (OOD) data. To generate OOD data we pick a random feature and split the data into the train set and OOD set by the median value on this feature. The experiments were run for 5 different splits. For OOD data good uncertainty estimates should have on average higher values compared to in-domain data. Table 2 provides for *concrete* dataset the percentages of OOD points with UE values higher than  $\alpha$  percentile of UE distribution for training data ( $\alpha = 80\%, 90\%, 95\%$ ). The resulting numbers should be considered with a significant

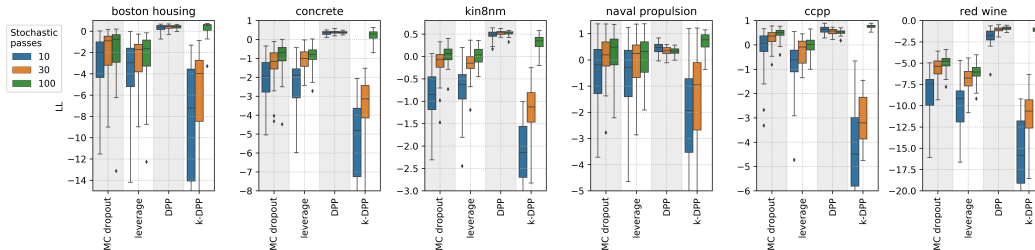


Figure 2: Log-likelihood metric across various UCI datasets for NN UE models with different number of stochastic passes  $T = 10, 30, 100$ . DPP and k-DPP give better results compared to other methods with DPP working well already for  $T = 10$  and consistently showing lower variance.

Table 2: Percentages of OOD points with UE values higher than specified percentile of UE distribution for training data for *concrete* dataset. DPP and k-DPP show the best results based on average values (top-2 average values are put in **bold**). For all the methods  $T = 100$ .

percentile	MC dropout	leverage	DPP	k-DPP
80	55.0±27.6	61.3±27.7	<b>70.4±26.0</b>	<b>71.9±28.0</b>
90	46.0±30.7	52.9±30.8	<b>59.6±30.1</b>	<b>60.8±33.7</b>
95	40.6±32.1	46.5±33.1	<b>52.1±32.9</b>	<b>51.8±36.3</b>

grain of salt due to their high variance but still DPP and k-DPP show the best results based on average values. Supplementary Material provides the results of OOD experiment for other datasets.

### 3.2 Uncertainty Estimation for Classification

#### 3.2.1 Data, Models and Metrics

In this section, we aim to show the applicability of the proposed methods to the classification tasks. We take *BALD* [Houlsby et al., 2011] as an uncertainty estimate. We consider three datasets: MNIST, which is a toy dataset of handwritten digits [LeCun, 1998], CIFAR-10, which is a 10-class image dataset with simple objects [Krizhevsky et al., 2009], and ImageNet [Deng et al., 2009], the large scale image classification dataset. Importantly, for MNIST we use only 500 train samples, otherwise the models would have too good accuracy and uncertainty estimation for in-domain data would not be relevant. For CIFAR-10 we use 50'000 samples for training and 10'000 for testing. For the MNIST dataset, we use a simple convolutional neural network with two convolutional layers, max-pooling and two fully connected layers. For the CIFAR-10 we use a more powerful network with 6 convolutional layers and batch normalization. Finally, for ImageNet we use the pre-trained ResNet-18 neural network [He et al., 2016] from PyTorch [Paszke et al., 2019]. Dropout with rate  $p = 0.5$  is used before the last fully-connected layer in all the cases.  $T = 100$  stochastic passes were made for every model. The experiments are repeated three times with different seeds for the models.

#### 3.2.2 Experimental Results

For in-domain uncertainty estimation the results are presented via UE-accuracy curve, see Figure 3. It assumes that samples with lower uncertainty will be classified with a higher average accuracy. It can be clearly seen that DPP significantly outperforms all the competitors on every dataset. We should emphasize that the superiority of DPP is especially strong for ImageNet, where the usage of DPP required only 2% computational overhead compared to MC dropout according to our experiments.

We also consider detection of out-of-distribution samples which is one of the important problems for the uncertainty estimation. As OOD samples we use fashion-MNIST [Xiao et al., 2017] and SVHN images [Netzer et al., 2011] for MNIST and CIFAR-10 correspondingly. We use count-vs-uncertainty curve and expect there should be few points with the low uncertainty for good uncertainty estimation methods. The results are presented in Figure 4. We see that DPP-based approach allows to detect the OOD samples better for the both considered datasets.

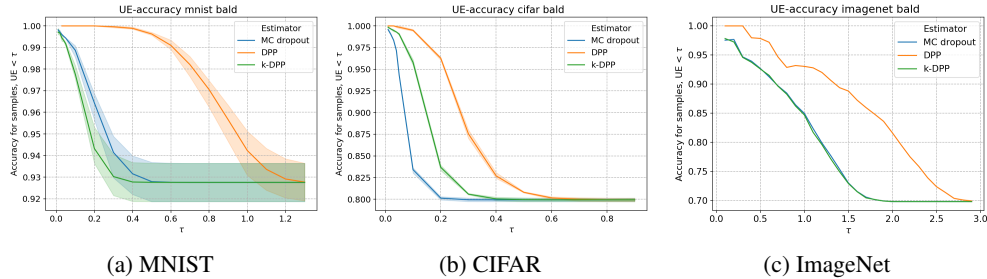


Figure 3: UE-accuracy curve (the higher curve – the better). We select the samples with low uncertainty to assure that the accuracy is higher for them.

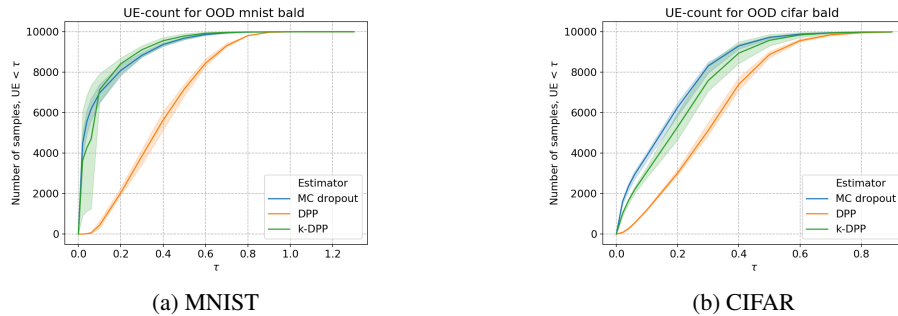


Figure 4: Count-vs-uncertainty curve for out-of-distribution data (the lower curve – the better).

## 4 Related Work

Dropout [Hinton et al., 2012, Srivastava et al., 2014] has emerged in recent years as a technique to prevent the overfitting in deep and overparametrized neural networks. Over the years, it obtained theoretical explanations as an averaged ensembling technique [Srivastava et al., 2014], a Bernoulli realization of the corresponding Bayesian neural network [Gal and Ghahramani, 2016] and a latent variable model [Maeda, 2014]. It was shown in [Gal, 2016, Nalisnick et al., 2019] that using dropout at the prediction stage (i.e., stochastic forward passes of the test samples through the network, also referred to as *MC dropout*) leads to unbiased Monte-Carlo estimates of the mean and variance for the corresponding Bayesian neural network trained using variational inference. These uncertainty estimates were shown to be efficient in different scenarios [Gal, 2016, Tsymbalov et al., 2018].

Training an ensemble of models and uncertainty estimation by their disagreement is another common approach [Lakshminarayanan et al., 2017]. It is shown that with few models in an ensemble, you can get robust and useful calibrated results [Beluch et al., 2018], outperforming MC dropout in active learning and error detection. The main disadvantage of ensembles is the necessity to train multiple model instances. However, it was addressed in recent works [Maddox et al., 2019, Garipov et al., 2018, Izmailov et al., 2019] which consider different strategies for speeding up ensemble construction. Recently, it was shown that improving diversity of ensemble members improves the quality of the resulting uncertainty estimates [Jain et al., 2019]. We also mention recent works which thoroughly investigate in-domain [Ashukha et al., 2020] and out-of-domain [Snoek et al., 2019] uncertainty estimation in classification for the case of maximum probability uncertainty estimate.

## 5 Conclusions

We have proposed a new approach that strengthens the dropout-based uncertainty estimation for neural networks. Instead of randomly sampling the dropout masks on the inference stage, we sample special sets of diverse neurons via determinantal point processes that utilize the information about the correlations of neurons in the inner layers. Numerical experiments on a wide range of regression and

classification tasks show that uncertainty estimates based on our approach outperform the MC dropout and other baselines with a significant margin. From the practical perspective, our method is simple to implement as it does not require any modifications to the neural network architecture and the training process. Importantly, the proposed uncertainty estimates have high quality even for a small number of stochastic passes through the network making the inference stage even faster in practice.

We expect that the proposed methods of dropout mask sampling may also be used on the training stage, leading to more robust and efficient models. Another compelling direction of further research is approximate DPP sampling, which may increase the sampling speed of the proposed approaches, making them more production-friendly.

## Acknowledgements

The authors want to thank Nikita Mokrov for useful discussions. E.T. was supported by the Skoltech NGP Program No. 2016-7/NGP (a Skoltech-MIT joint project) and by the Center for Integrated Nanotechnologies, an Office of Science User Facility operated for the U.S. Department of Energy (DOE) Office of Science by Los Alamos National Laboratory (Contract 89233218CNA000001) and Sandia National Laboratories (Contract DE-NA-0003525). E.T. also acknowledges the usage of the Magnus computational platform by the Skoltech CEST Multiscale Molecular Modelling group (Prof. Alexander Shapeev) for obtaining the part of results presented in this paper. M.P. and K.F. acknowledge the use of “Zhores” supercomputer [Zacharov et al., 2019] for obtaining the part of results presented in this paper.

## Broader Impact

In a number of application areas, such as engineering design, detection of breaks, personalized medicine, and many others, it is critically important to accurately assess the model prediction error so that conclusions about its applicability can be made for each specific prediction. Moreover, for a number of the most widely used machine learning algorithms, such as neural networks, at the moment there are no reliable and accurate estimates of prediction errors, and obtaining them is a difficult task from a scientific point of view. Moreover, estimates of prediction errors are important tools in solving the problems of experiment planning and Bayesian optimization, which are widely in demand in modern applications. Thus, the estimation of expected prediction errors or, more broadly, the estimation of prediction uncertainty is an important problem, the solution of which will significantly expand the applicability of neural network machine learning algorithms, as well as bring these algorithms closer to reliable engineering tools for solving applied problems.

Speaking about our approach, we, of course, don't claim that it solves the problem in full. However, the important property of our approach is that for the wide class of neural networks used in practice, it doesn't require any modifications to network architecture and training process. Thus, our approach is easily applicable, while providing considerably improved quality of uncertainty estimation.

## References

- [Alaoui and Mahoney, 2015] Alaoui, A. and Mahoney, M. W. (2015). Fast randomized kernel ridge regression with statistical guarantees. In *Advances in Neural Information Processing Systems*, pages 775–783.
- [Amblard et al., 2018] Amblard, P.-O., Barthelmé, S., and Tremblay, N. (2018). Subsampling with  $k$  determinantal point processes for estimating statistics in large data sets. In *2018 IEEE Statistical Signal Processing Workshop (SSP)*, pages 313–317. IEEE.
- [Ashukha et al., 2020] Ashukha, A., Lyzhov, A., Molchanov, D., and Vetrov, D. (2020). Pitfalls of in-domain uncertainty estimation and ensembling in deep learning. *arXiv preprint arXiv:2002.06470*.
- [Begoli et al., 2019] Begoli, E., Bhattacharya, T., and Kusnezov, D. (2019). The need for uncertainty quantification in machine-assisted medical decision making. *Nature Machine Intelligence*, 1(1):20–23.
- [Beluch et al., 2018] Beluch, W. H., Genewein, T., Nürnberger, A., and Köhler, J. M. (2018). The power of ensembles for active learning in image classification. In *Proceedings CVPR*, pages 9368–9377.

- [Çivril and Magdon-Ismail, 2009] Çivril, A. and Magdon-Ismail, M. (2009). On selecting a maximum volume sub-matrix of a matrix and related problems. *Theoretical Computer Science*, 410(47-49):4801–4811.
- [Deng et al., 2009] Deng, J., Dong, W., Socher, R., Li, L.-J., Li, K., and Fei-Fei, L. (2009). Imagenet: A large-scale hierarchical image database. In *2009 IEEE conference on computer vision and pattern recognition*, pages 248–255. Ieee.
- [Dua and Taniskidou, 2017] Dua, D. and Taniskidou, E. K. (2017). Uci machine learning repository [<http://archive.ics.uci.edu/ml>].
- [Feng et al., 2018] Feng, D., Rosenbaum, L., and Dietmayer, K. (2018). Towards safe autonomous driving: Capture uncertainty in the deep neural network for lidar 3d vehicle detection. In *21st International Conference on Intelligent Transportation Systems (ITSC)*, pages 3266–3273.
- [Freeman, 1965] Freeman, L. C. (1965). *Elementary applied statistics: for students in behavioral science*. John Wiley & Sons.
- [Gal, 2016] Gal, Y. (2016). Uncertainty in deep learning. *University of Cambridge*.
- [Gal and Ghahramani, 2016] Gal, Y. and Ghahramani, Z. (2016). Dropout as a bayesian approximation: Representing model uncertainty in deep learning. In *Proc. ICML'16*, pages 1050–1059.
- [Gal et al., 2017] Gal, Y., Islam, R., and Ghahramani, Z. (2017). Deep bayesian active learning with image data. In *Proceedings of the 34th International Conference on Machine Learning-Volume 70*, pages 1183–1192.
- [Garipov et al., 2018] Garipov, T., Izmailov, P., Podoprikin, D., Vetrov, D. P., and Wilson, A. G. (2018). Loss surfaces, mode connectivity, and fast ensembling of dnns. In *Advances in Neural Information Processing Systems*, pages 8789–8798.
- [Gautier et al., 2019] Gautier, G., Polito, G., Bardenet, R., and Valko, M. (2019). Dppy: Dpp sampling with python. *JMLR*, 20(180):1–7.
- [Goreinov et al., 2010] Goreinov, S. A., Oseledets, I. V., Savostyanov, D. V., Tyrtshnikov, E. E., and Zamarashkin, N. L. (2010). How to find a good submatrix. In *Matrix Methods: Theory, Algorithms And Applications: Dedicated to the Memory of Gene Golub*, pages 247–256. World Scientific.
- [Guo et al., 2017] Guo, C., Pleiss, G., Sun, Y., and Weinberger, K. Q. (2017). On calibration of modern neural networks. In *Proceedings ICML*, page 1321–1330.
- [He et al., 2016] He, K., Zhang, X., Ren, S., and Sun, J. (2016). Deep residual learning for image recognition. In *Proceedings of the IEEE conference on computer vision and pattern recognition*, pages 770–778.
- [Hein et al., 2019] Hein, M., Andriushchenko, M., and Bitterwolf, J. (2019). Why relu networks yield high-confidence predictions far away from the training data and how to mitigate the problem. In *Proceedings of the IEEE Conference on Computer Vision and Pattern Recognition*, pages 41–50.
- [Hernández-Lobato and Adams, 2015] Hernández-Lobato, J. M. and Adams, R. (2015). Probabilistic backpropagation for scalable learning of bayesian neural networks. In *International Conference on Machine Learning*, pages 1861–1869.
- [Hinton et al., 2012] Hinton, G. E., Srivastava, N., Krizhevsky, A., Sutskever, I., and Salakhutdinov, R. R. (2012). Improving neural networks by preventing co-adaptation of feature detectors. *arXiv:1207.0580*.
- [Horvitz and Thompson, 1952] Horvitz, D. G. and Thompson, D. J. (1952). A generalization of sampling without replacement from a finite universe. *Journal of the American statistical Association*, 47(260):663–685.
- [Houlsby et al., 2011] Houlsby, N., Huszár, F., Ghahramani, Z., and Lengyel, M. (2011). Bayesian active learning for classification and preference learning. *arXiv preprint arXiv:1112.5745*.
- [Irvin et al., 2019] Irvin, J., Rajpurkar, P., Ko, M., Yu, Y., Ciurea-Ilcus, S., Chute, C., Marklund, H., Haghighi, B., Ball, R., Shpanskaya, K., et al. (2019). Chexpert: A large chest radiograph dataset with uncertainty labels and expert comparison. In *Proceedings of the AAAI Conference on Artificial Intelligence*, volume 33, pages 590–597.
- [Izmailov et al., 2019] Izmailov, P., Maddox, W., Kirichenko, P., Garipov, T., Vetrov, D., and Wilson, A. G. (2019). Subspace inference for bayesian deep learning.

- [Jain et al., 2019] Jain, S., Liu, G., Mueller, J., and Gifford, D. (2019). Maximizing overall diversity for improved uncertainty estimates in deep ensembles. *arXiv preprint arXiv:1906.07380*.
- [Krizhevsky et al., 2009] Krizhevsky, A., Hinton, G., et al. (2009). Learning multiple layers of features from tiny images.
- [Kulesza et al., 2012] Kulesza, A., Taskar, B., et al. (2012). Determinantal point processes for machine learning. *Foundations and Trends® in Machine Learning*, 5(2–3):123–286.
- [Lakshminarayanan et al., 2017] Lakshminarayanan, B., Pritzel, A., and Blundell, C. (2017). Simple and scalable predictive uncertainty estimation using deep ensembles. In *Advances in neural information processing systems*, pages 6402–6413.
- [LeCun, 1998] LeCun, Y. (1998). The mnist database of handwritten digits. <http://yann.lecun.com/exdb/mnist/>.
- [Maas et al., 2013] Maas, A. L., Hannun, A. Y., and Ng, A. Y. (2013). Rectifier nonlinearities improve neural network acoustic models. In *Proc. ICML'13*, volume 30, page 3.
- [Macchi, 1975] Macchi, O. (1975). The coincidence approach to stochastic point processes. *Advances in Applied Probability*, 7(1):83–122.
- [Maddox et al., 2019] Maddox, W. J., Izmailov, P., Garipov, T., Vetrov, D. P., and Wilson, A. G. (2019). A simple baseline for bayesian uncertainty in deep learning. In *NeurIPS*, pages 13132–13143.
- [Maeda, 2014] Maeda, S.-i. (2014). A bayesian encourages dropout. *arXiv:1412.7003*.
- [Nalisnick et al., 2019] Nalisnick, E., Hernandez-Lobato, J. M., and Smyth, P. (2019). Dropout as a structured shrinkage prior. In *International Conference on Machine Learning*, pages 4712–4722.
- [Netzer et al., 2011] Netzer, Y., Wang, T., Coates, A., Bissacco, A., Wu, B., and Ng, A. Y. (2011). Reading digits in natural images with unsupervised feature learning.
- [Paszke et al., 2019] Paszke, A., Gross, S., Massa, F., Lerer, A., Bradbury, J., Chanan, G., Killeen, T., Lin, Z., Gimelshein, N., Antiga, L., Desmaison, A., Kopf, A., Yang, E., DeVito, Z., Raison, M., Tejani, A., Chilamkurthy, S., Steiner, B., Fang, L., Bai, J., and Chintala, S. (2019). Pytorch: An imperative style, high-performance deep learning library. In Wallach, H., Larochelle, H., Beygelzimer, A., d’Álché-Buc, F., Fox, E., and Garnett, R., editors, *Advances in Neural Information Processing Systems 32*, pages 8024–8035. Curran Associates, Inc.
- [Settles, 2012] Settles, B. (2012). Active learning. *Synthesis Lectures on Artificial Intelligence and Machine Learning*, 6(1):1–114.
- [Smith et al., 2018] Smith, J. S., Nebgen, B., Lubbers, N., Isayev, O., and Roitberg, A. E. (2018). Less is more: Sampling chemical space with active learning. *The Journal of chemical physics*, 148(24):241733.
- [Snoek et al., 2019] Snoek, J., Oquendo, Y., Fertig, E., Lakshminarayanan, B., Nowozin, S., Sculley, D., Dillon, J., Ren, J., and Nado, Z. (2019). Can you trust your model’s uncertainty? evaluating predictive uncertainty under dataset shift. In *Advances in Neural Information Processing Systems*, pages 13969–13980.
- [Srivastava et al., 2014] Srivastava, N., Hinton, G., Krizhevsky, A., Sutskever, I., and Salakhutdinov, R. (2014). Dropout: A simple way to prevent neural networks from overfitting. *The Journal of Machine Learning Research*, 15(1):1929–1958.
- [Tsybalov et al., 2018] Tsybalov, E., Panov, M., and Shapeev, A. (2018). Dropout-based active learning for regression. In *International Conference on Analysis of Images, Social Networks and Texts*, pages 247–258.
- [Vyas et al., 2018] Vyas, A., Jammalamadaka, N., Zhu, X., Das, D., Kaul, B., and Willke, T. L. (2018). Out-of-distribution detection using an ensemble of self supervised leave-out classifiers. In *Proceedings ECCV*, pages 550–564.
- [Xiao et al., 2017] Xiao, H., Rasul, K., and Vollgraf, R. (2017). Fashion-mnist: a novel image dataset for benchmarking machine learning algorithms.
- [Zacharov et al., 2019] Zacharov, I., Arslanov, R., Gunin, M., Stefonishin, D., Bykov, A., Pavlov, S., Panarin, O., Maliutin, A., Rykovanov, S., and Fedorov, M. (2019). “zhores”—petaflops supercomputer for data-driven modeling, machine learning and artificial intelligence installed in skolkovo institute of science and technology. *Open Engineering*, 9(1):512–520.

# Supplementary Material

## A Regression Experiments

### A.1 Details on Model Training

Neural networks were trained for  $10^4$ 000 epochs maximum, with checking the error on the validation set every 100 iterations: early stopping triggers if the error did not decrease for a five consecutive checks (patience = 5). Batch size equals to 500, dropout applied after the hidden layers only (except for the last layer) with rate equal to 0.5, except for the experiment C (see below). MSE was used as a loss function, and optimization was performed with the standard settings of PyTorch Adadelata optimizer. For the details on activation function and architecture please refer to Table 5, which summarizes the architectures we used (referred as Experiments A, B, C and D).

Ensembles of models were trained separately on the same data from different random weight initializations.

### A.2 Experiments with Ensembles

We start with the Experiment A (the same as in the main text), consider ensembles of 5 models and combine them with the different inference methods for individual models. We visualize the log-likelihood metric for each dataset, see Figure 5. There is no single method which gives the best results uniformly over the considered datasets, yet DPP-based methods show superior performance more often than other approaches. Also it is clearly seen that pure ensembling without sampling in individual models is usually inferior even to the plain MC dropout, while combination of ensembling with sampling consistently improves the quality of uncertainty estimation.

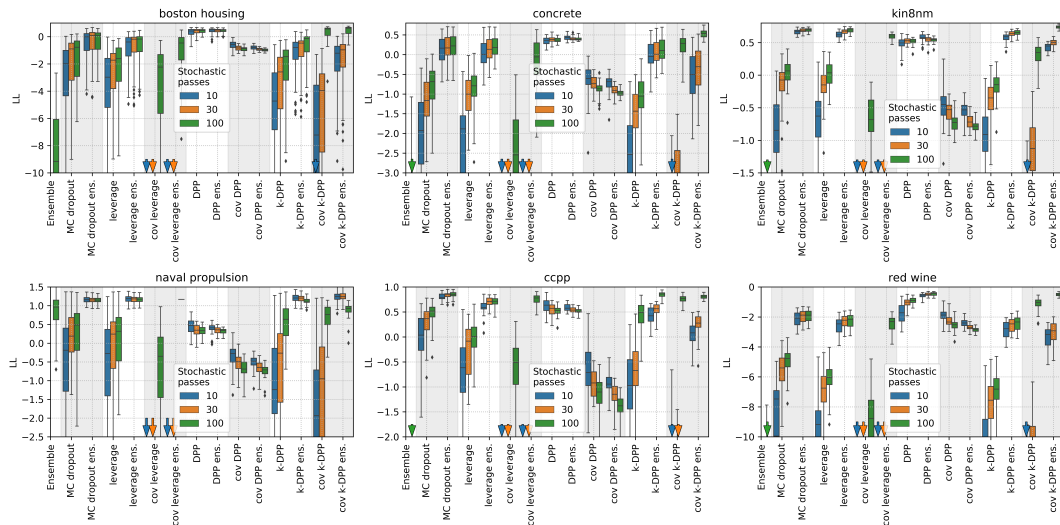


Figure 5: Log-likelihood across various UCI datasets for single models and ensembles of NN UE models. Arrows on the bottom indicate box plots being below the bottom boundary. DPP constantly shows good results in the single model scenario, being not far from ensemble-based methods.

### A.3 OOD Results for Other Datasets

Tables 3 and 4 provide percentages of OOD points with UE values higher than  $\alpha$  percentile of UE distribution for training data ( $\alpha = 80\%, 90\%, 95\%$ ) for two other datasets: *Boston housing* and *red wine*. As for the similar experiment in main text, the resulting numbers should be considered with a significant grain of salt due to their high variance but still DPP and k-DPP show the best results based on average values.

Table 3: Percentages of OOD points with UE values higher than specified percentile of UE distribution for training data for *Boston housing* dataset. DPP and k-DPP show the best results based on average values (top-2 average values are put in **bold**). For all the methods,  $T = 100$ .

percentile	MC dropout	leverage	DPP	k-DPP
80	49.6±26.9	68.1±23.7	<b>69.2±29.3</b>	<b>83.1±23.2</b>
90	36.9±27.9	53.6±26.9	<b>59.6±31.5</b>	<b>63.7±29.4</b>
95	28.2±26.7	40.7±30.0	<b>53.5±32.5</b>	<b>50.9±36.0</b>

Table 4: Percentages of OOD points with UE values higher than specified percentile of UE distribution for training data for *red wine* dataset. DPP and k-DPP show the best results based on average values (top-2 average values are put in **bold**). For all the methods,  $T = 100$ .

percentile	MC dropout	leverage	DPP	k-DPP
80	50.4±26.9	53.1±22.3	<b>73.5±23.9</b>	<b>60.9±26.5</b>
90	36.6±28.0	39.1±23.5	<b>61.8±29.2</b>	<b>45.0±31.1</b>
95	27.3±27.7	30.1±22.6	<b>51.0±31.9</b>	<b>34.7±34.2</b>

#### A.4 Experiments with Different NN architectures

In order to test the robustness of the obtained results with respect to changes of NN architecture and other parameters, we settled out three more experiments with variations in:

- **architecture.** Different problems may require different number and different size of fully-connected layers of NNs to be used in order to being able fit the train data well and do not overfit.
- **activation function.** It was shown [Hein et al., 2019] that the choice of activation function may significantly influence the quality of uncertainty estimates. We consider ReLU and CELU activation functions.
- **dropout rate.** While usually in the literature the dropout rate  $p = 0.5$  is often considered, for real problems lesser values of  $p$  are often used in order to speed up the convergence. For example, , the dropout rate is proposed to be chosen in a cross-validation round [Gal, 2016] together with other hyperparameters, such as regularization weight, learning rate, etc. In this work, we simply try other dropout value to check the robustness with respect to the change of this parameter.

The variations in the settings are provided in Table 5, with the results of Experiment A provided in the main text.

Table 5: Settings for UCI experiments.

Index	Architecture	Activation	$p$
A (main text)	128-128-64	leaky ReLU	0.5
B	32-32-16	leaky ReLU	0.5
C	128-128-256	CELU	0.2
D	256-256-512	CELU	0.5

We have visualized the results for other experiments in Figures 6, 7 and 8. DPP-based methods show the best performance for majority of cases. For the very large (relatively to the datasets size) NN architecture, leverage score-based approach shows promising performance as well.

## B Classification Experiments

### B.1 Details on Models Training

In the classification tasks, neural networks were trained for 100 epochs maximum, with checking the error on the validation set every epoch: early stopping triggers if the error did not decrease for

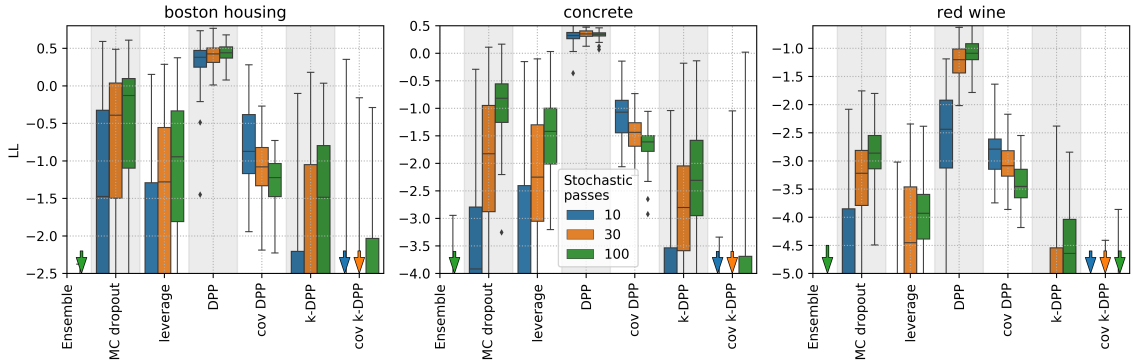


Figure 6: Log-likelihood across various UCI datasets for single models of NN UE for the small-NN experiment B, see Table 5 for setup details. DPP shows outstanding performance; it also demonstrates the most stable results in terms of the variance between the runs. Arrows on the bottom indicate box plots being below the bottom boundary.

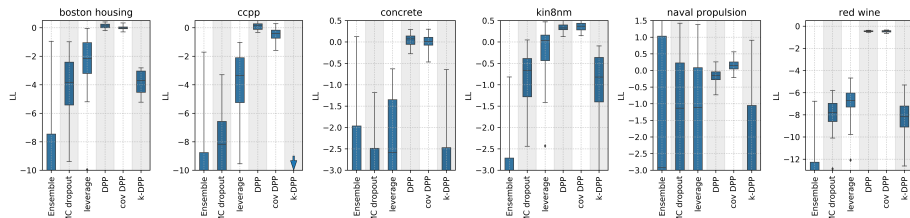


Figure 7: Log-likelihood across various UCI datasets for single models of NN UE for the large-NN experiment C with the reduced dropout rate, see Table 5 for setup details. Larger number of stochastic runs (30, 100) demonstrate the performance inferior to the 10 runs approach. DPP and k-DPP methods show stable dominance over other approaches. Arrows on the bottom indicate box plots being below the bottom boundary.

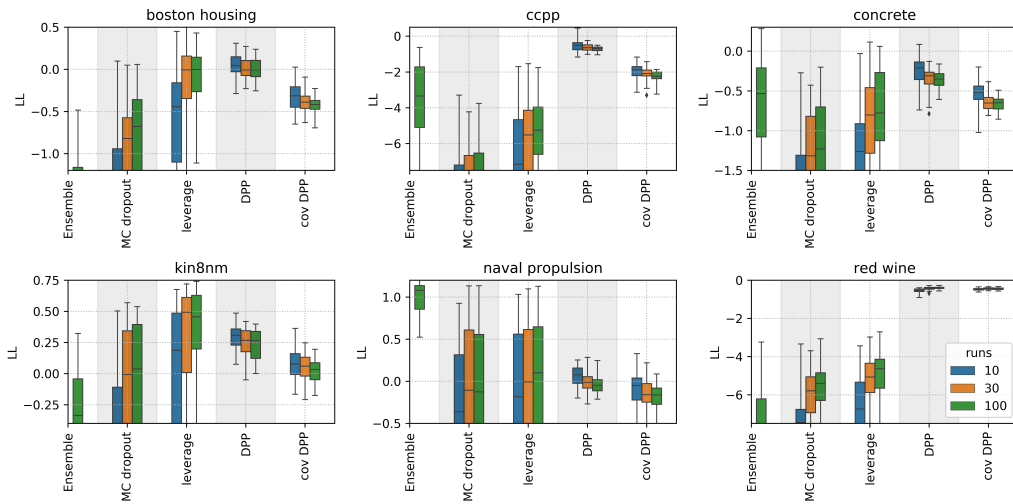


Figure 8: Log-likelihood across various UCI datasets for single models of NN UE for the large-NN experiment D, see Table 5 for setup details. DPP and leverage mask decorrelation shows the best results. Arrows on the bottom indicate box plots being below the bottom boundary.

three consecutive checks (patience = 3). Batch size equals to 128, dropout applied after the hidden linear layer with a rate equal to 0.5. Cross entropy was used as a loss function, and optimization was

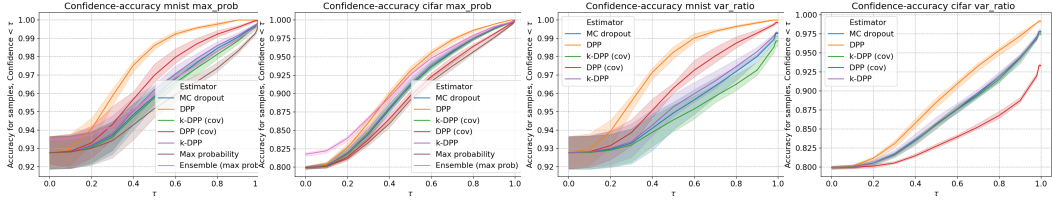


Figure 9: Accuracy-vs-confidence curve (the higher curve – the better). We provide results for max probability and variation ratio measures for MNIST and CIFAR datasets.

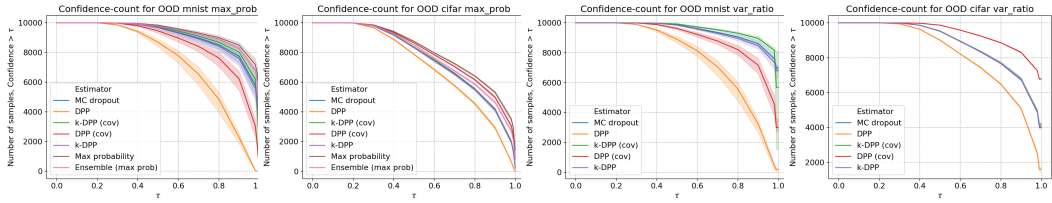


Figure 10: Count-vs-confidence curve for out-of-distribution data (the lower curve – the better). We provide results for max probability and variation ratio measures for MNIST and CIFAR datasets.

performed with the standard setting of PyTorch Adam optimizer. For each dataset, we use different models. Below we denote convolutional layer with  $i$  input channels,  $j$  output channels as  $\text{conv}(i, j)$ . Kernel size is  $3 \times 3$  for each convolution.

- For the MNIST, we used simple convolutional network with layers  $\text{conv}(1, 16)$  - maxpool -  $\text{conv}(16, 32)$  - maxpool - linear(1152, 256) - dropout - linear(256, 10)
- For the CIFAR, we used VGG-alike network with layers  $\text{conv}(3, 16)$  -  $\text{conv}(16, 16)$  - maxpool(2, 2) -  $\text{conv}(16, 32)$  -  $\text{conv}(32, 32)$  - maxpool(2, 2) -  $\text{conv}(32, 64)$  -  $\text{conv}(64, 64)$  - maxpool(2, 2) - linear(1024, 128) - dropout - linear(128, 10)
- For the ImageNet, we used ResNet-18 with implementation and pretrained weights from PyTorch.

Ensembles of models for experiments below were trained separately on the same data from different weight initializations.

## B.2 Different Uncertainty Estimation Methods

For classification, one could use different uncertainty estimation measures. In the main part of the paper we provided results for BALD. The other popular uncertainty measures in the literature are

- **1 - maximum probability:** simple averaging of probabilities over the ensemble and taking the one with maximum value:  $s(\mathbf{x}) = 1 - \max_c \bar{p}_T(y = c | \mathbf{x})$
- **Variation ratio:**  $v(\mathbf{x}) = 1 - \frac{f_m(\mathbf{x})}{T}$ , where  $f_m(\mathbf{x})$  is the number of predictions for the most frequently chosen class by distinct runs of the model or members of the ensemble.

In this section, we provide the results for these two methods (see Figure 9). For the probability, we average the predictions for all dropout masks. We also report the result for a single network without a dropout and for an ensemble of 20 independently trained networks. The same methods are applied for the OOD experiment (Figure 10). Note, here we provide the results for our methods both with correlation and covariance (cov) kernels. We can see that for these measures our DPP approach based on the correlation kernel outperforms the other approaches as well.

## B.3 ImageNet OOD Experiment

We present the out-of-distribution experiment for the ImageNet dataset here. As OOD images, we took the 50'000 samples from the CheXpert Small(chest radiography dataset) [Irvin et al., 2019]. We

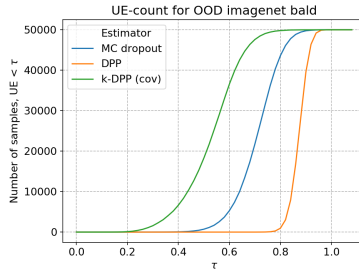


Figure 11: Count-vs-uncertainty curve for out-of-distribution data on ImageNet (the lower curve – the better).

used BALD uncertainty measure, the same as in the main part of the paper. The results are presented on Figure 11. The DPP method performs very well, while k-DPP is inferior to the MC Dropout.

#### B.4 Scalability notes

One of our initial concerns was the scalability of the methods because DPP sampling complexity is up to  $N^3$ , where  $N$  is the size of the layer. In practice, the overhead appears to be relatively small for real-world models, because the number of operations to compute dropout masks is negligible compared to the normal forward propagation in a large network. For the ImageNet experiment the difference was less than a few percent comparing to the Monte-Carlo dropout, see Table 6.

Table 6: Time to calculate uncertainty with different methods on 5'000 sample images from ImageNet

	MC dropout	DPP	k-DPP
Inference time, s	125.5±0.03	129.9±0.14	132.2±0.03